

Supplementary Information

Enhancing Charge Transfer with Foreign Molecules through Femtosecond Laser Induced MoS₂ Defect Sites for Photoluminescence Control and SERS Enhancement

Pei Zuo,^a Lan Jiang,^{*,a} Xin Li,^a Peng Ran,^a Bo Li,^a Aisheng Song,^b Mengyao Tian,^a Tianbao Ma,^b Baoshan Guo,^a Liangti Qu^{c,d} and Yongfeng Lu^e

^aLaser Micro/Nano Fabrication Laboratory, School of Mechanical Engineering, Beijing Institute of Technology, Beijing 100081, P.R. China,

^bState Key Laboratory of Tribology, Tsinghua University, Beijing 100084, P.R. China,

^cKey Laboratory for Advanced Materials Processing Technology, Ministry of Education of China, Tsinghua University, Beijing 100084, P.R. China,

^dBeijing Key Laboratory of Photoelectronic/Electrophotonic Conversion Materials, Key Laboratory of Cluster Science, School of Chemistry, Beijing Institute of Technology, Beijing 100081, P.R. China,

^eDepartment of Electrical and Computer Engineering, University of Nebraska-Lincoln, Lincoln, NE 68588-0511, USA

**Address correspondence to jianglan@bit.edu.cn*

Supplementary figures and table

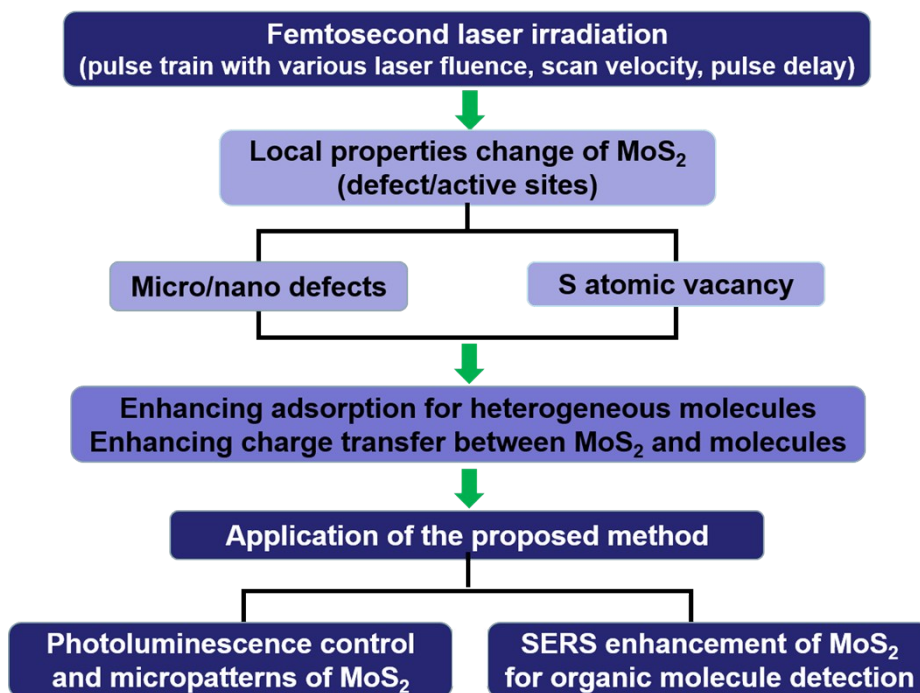


Fig. S1 Structure of this work.

Table S1 All the abbreviations and the corresponding full names.

Abbreviations	Full names
TMDs	transition-metal dichalcogenides
2D	two-dimensional
MoS ₂	molybdenum disulfide
CFL	conventional femtosecond laser
TSFL	temporally shaped femtosecond laser
FLT	femtosecond laser-treated
CFLT	conventional femtosecond laser-treated
TSFLT	temporally shaped femtosecond laser-treated
P-MoS₂	pristine MoS₂
FLT-MoS₂	femtosecond laser-treated MoS₂
CFLT- MoS₂	conventional femtosecond laser-treated MoS₂
TSFLT- MoS₂	temporally shaped femtosecond laser-treated MoS₂
CVD	chemical vapour deposition

OL	objective lens
TPA	two-photon absorption
AFM	Atomic force microscope
SEM	scanning electron microscope
XPS	X-ray photoelectron spectroscopy
DFT	density functional theory
O ₂	oxygen
R6G	Rhodamine 6G
PL	photoluminescence
SERS	surface-enhanced-Raman-scattering
CM	chemical mechanism
EF	enhancement-factor
VASP	Vienna ab initio simulation package
PBE	Perdew–Burke–Ernzerhof

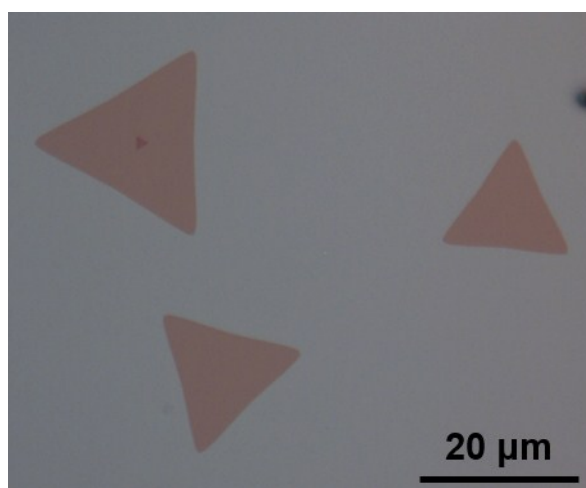


Fig. S2 Optical micrograph of triangular MoS₂ flakes grown and dispersive on substrate.

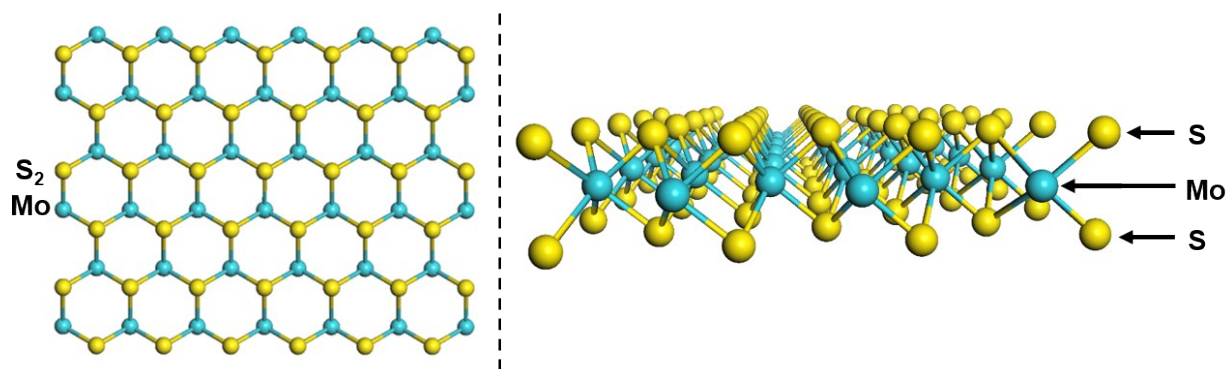


Fig. S3 Atomic structure (front and side views) of monolayer MoS₂.

The micromorphology (low and high resolution SEM images) of pristine MoS₂ flake are shown in Figure S4. They indicated that the surface of pristine MoS₂ was relatively smooth, clear, and flawless, when compared with the surface of femtosecond laser-treated MoS₂ flake (as shown in Figure 2), which provide the evidence that laser treatment caused these defect features of MoS₂.

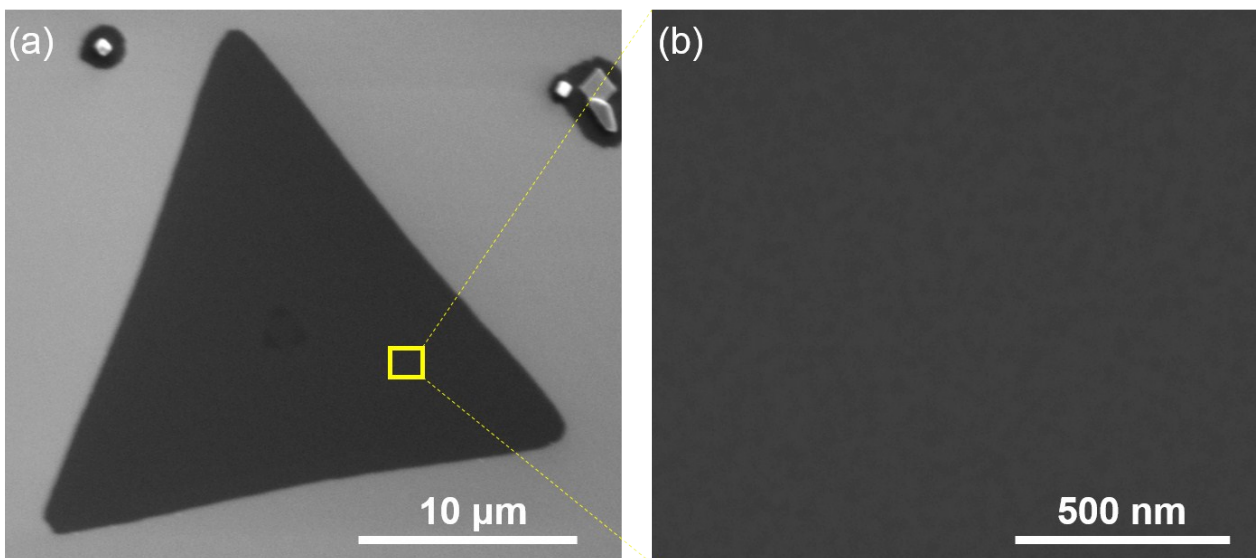


Fig. S4 Micromorphology of pristine MoS₂ flake. a) Low and b) high resolution SEM images of pristine MoS₂ flake.

Explanation for TSFLT, CFLT, and pulse delay.

Laser can be divided into continuous laser and pulsed laser according to its manner of working, among them, pulsed laser is the laser that operates as pulses, as shown in Figure S5. Femtosecond laser is a kind of pulsed laser with pulse width of femtosecond magnitude.

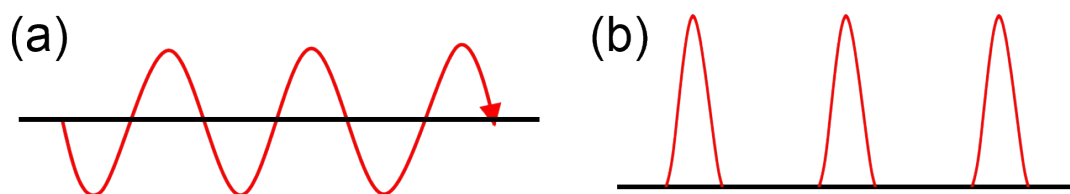


Fig. S5 Working manner of a) continuous laser and b) pulsed laser.

CFL represents conventional femtosecond laser, and TSFL represents temporally shaped femtosecond laser (conventional femtosecond pulse is temporally shaped into a pulse train), as shown in Figure S6. T is the time of pulse separation, which was 1 ms for the used femtosecond laser with pulse repetition frequency of 1KHz in our work. τ is the delay between two sub-pulses with energy ratio of 1:1 in our work, which is called “**pulse delay**”. CFL, no pulse delay, which is $\tau=0$ ps; TSFL, having pulse delay, which is $\tau>0$ ps.

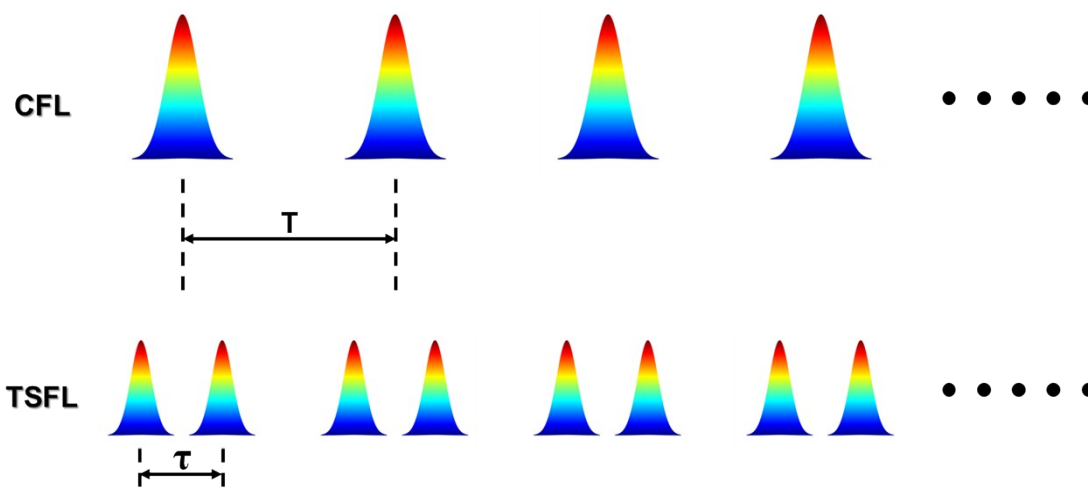


Fig. S6 Pulses of CFL and TSFL. T is the time of pulse separation, and τ is the delay between two sub-pulses, namely pulse delay.

In our work, the pulse delay was just one of the parameters of our femtosecond laser processing (pulse delay=0 ps, CFL; pulse delay>0 ps, TSFL). CFLT means CFL-treated, conventional femtosecond laser-treated; TSFLT means TSFL-treated, temporally shaped femtosecond laser-treated. CFLT-MoS₂ and TSFLT-MoS₂ were used when analyze the PL and SERS dependence on laser pulse delay, the purpose of which was to demonstrate the advantage of the improved temporally shaped femtosecond laser processing system, not only analyze the parameter

dependence. And the relationship between FLT, CFLT, TSFLT, and pulse delay is shown in Figure S7.

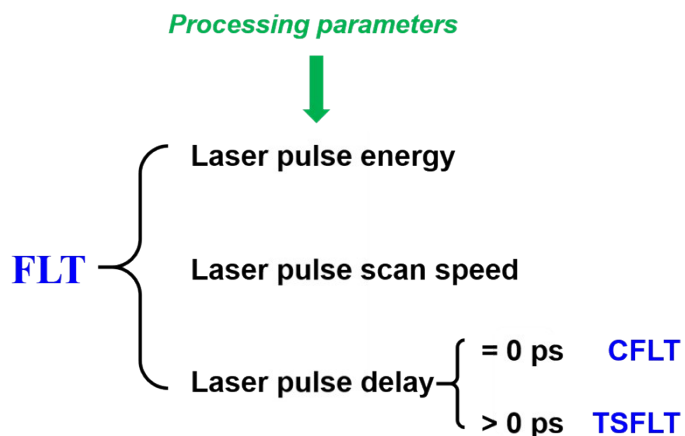


Figure S7 Relationship between FLT, CFLT, TSFLT, and pulse delay.

The local micromorphology of a FLT-MoS₂ flake is shown in Figure S8, which indicated the clear and uniform micro/nano defects on MoS₂ flake. In Figure S8a, the triangular region is a MoS₂ flake, the dot regions within triangular region are the fracture of MoS₂ where substrate can be seen. Figure S8b-f show the amplified images of different local regions of laser-treated MoS₂. In order to improve the definition and contrast of SEM images, we switched colors between MoS₂ and substrate. The light color regions are MoS₂, dark regions are many fractured-regions (structures) on MoS₂ where substrate can be seen, which is that dark regions are the exposed substrate. These defects such as micro/nano cracks and local damage are shown in Figure S8c-f. The size of microcracks and local microdamage was about 70~200 nm (Figure S8c and d), the width of threadlike nanocracks was about 15~50 nm (Figure S8d and e), and the size of local nanodamage introducing numerous MoS₂ nanosheets was about several~15 nm (Figure S8f).

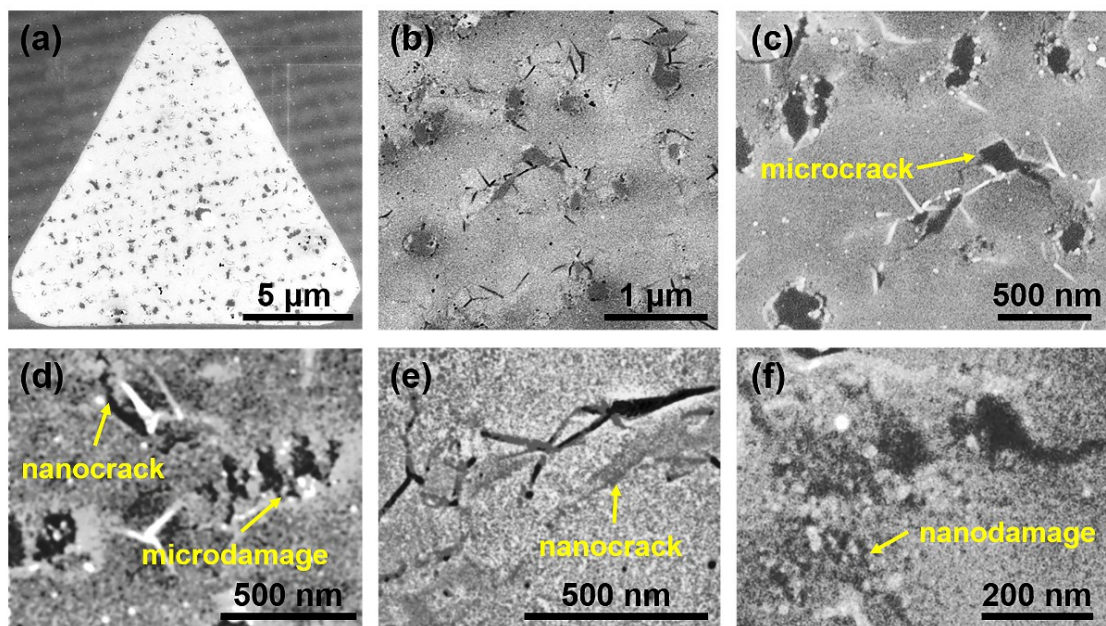


Fig. S8 Micro/nano defects on a FLT-MoS₂. SEM images of (a) a whole FLT-MoS₂ flake and the (b) local morphology of it. (c-f) High resolution SEM images of these defects such as micro/nano cracks and damages. The laser parameters for processing this FLT-MoS₂ was laser fluence of 0.43 J/cm², scan velocity of 500 μm/s and pulse delay of 1 ps.

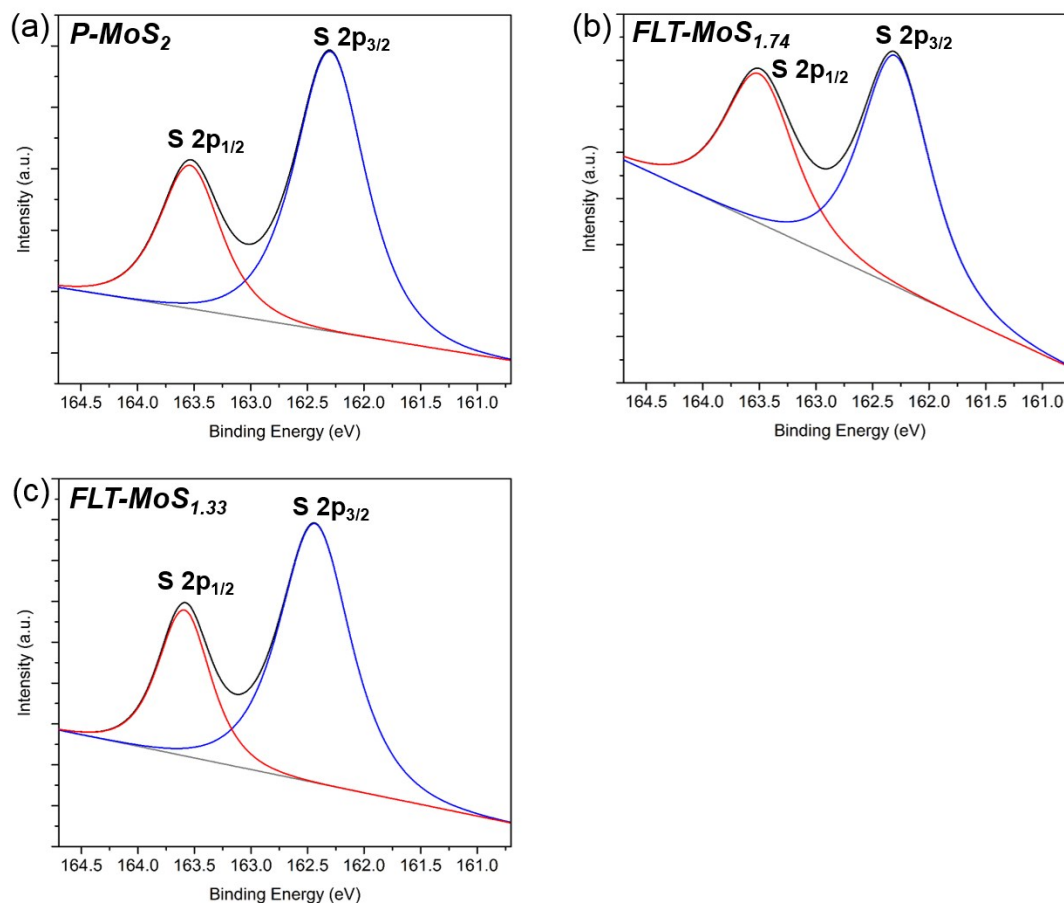


Fig. S9 XPS S 2p spectra of MoS₂ and two FLT-MoS₂ flakes. XPS S 2p spectra of (a) P-MoS₂, (b) FLT-MoS_{1.74} (parameters of laser irradiation were laser fluence of 0.43 J/cm², scan velocity of 500 μm/s, and pulse delay of 0 ps), and (c) FLT-MoS_{1.33} (parameters of laser irradiation were laser fluence of 0.64 J/cm², scan velocity of 300 μm/s, and pulse delay of 0 ps). It indicates that after laser treatment, no new peak (new binding energy of S) appeared, no old peak disappeared, and the peak positions did not obviously shift. Hence, no amorphous phase was present after laser treatment, and no crystalline sulfur were created after laser treatment, at least according to the XPS test and on the surface of laser-treated MoS₂ flakes.

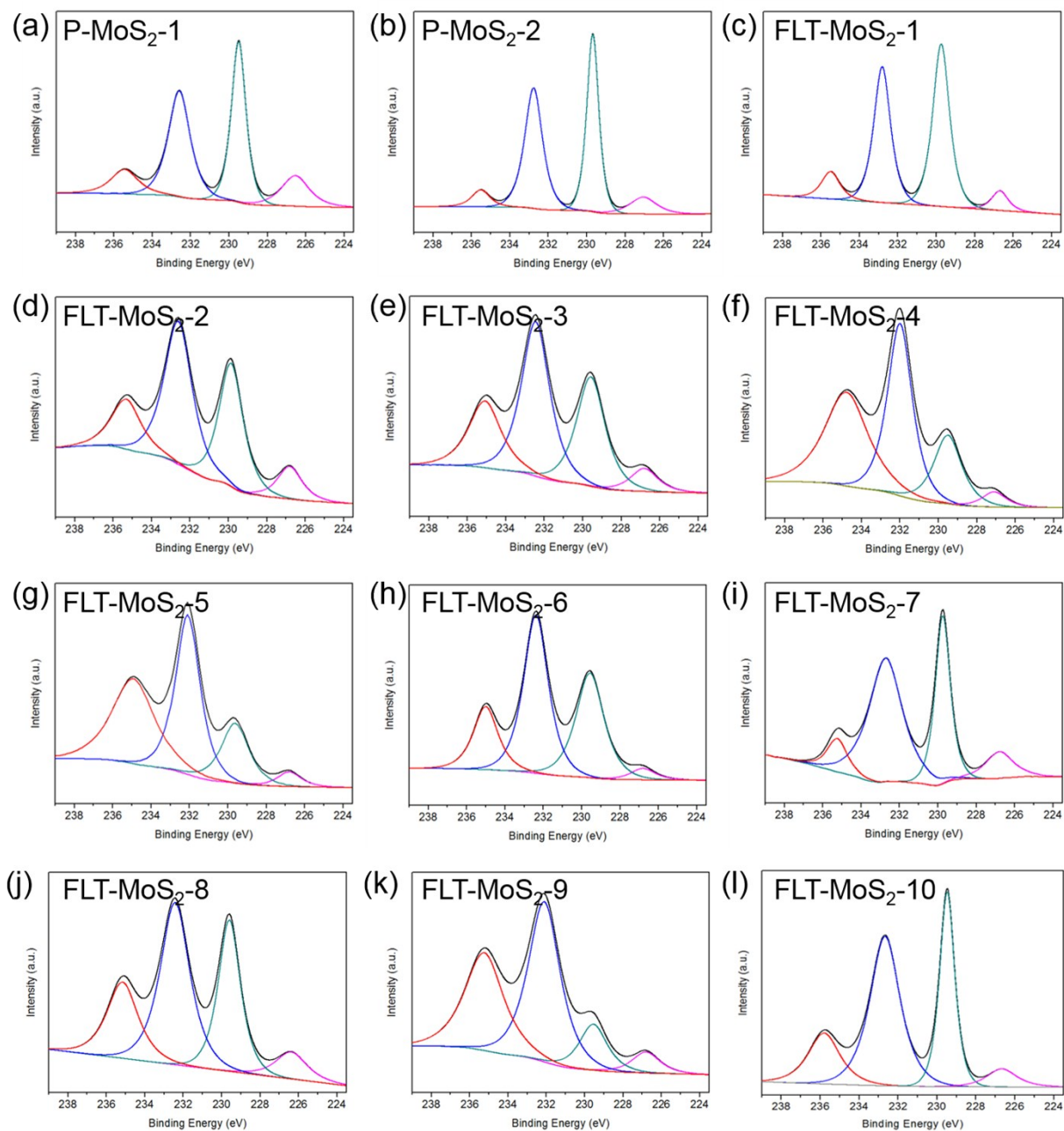


Fig. S10 More XPS Mo spectra of 2 P-MoS₂ and 10 FLT-MoS₂ samples. The red, blue, cyan, and magenta lines refer to Mo⁶⁺, Mo⁴⁺, Mo⁴⁺, and S 2s peaks, respectively.

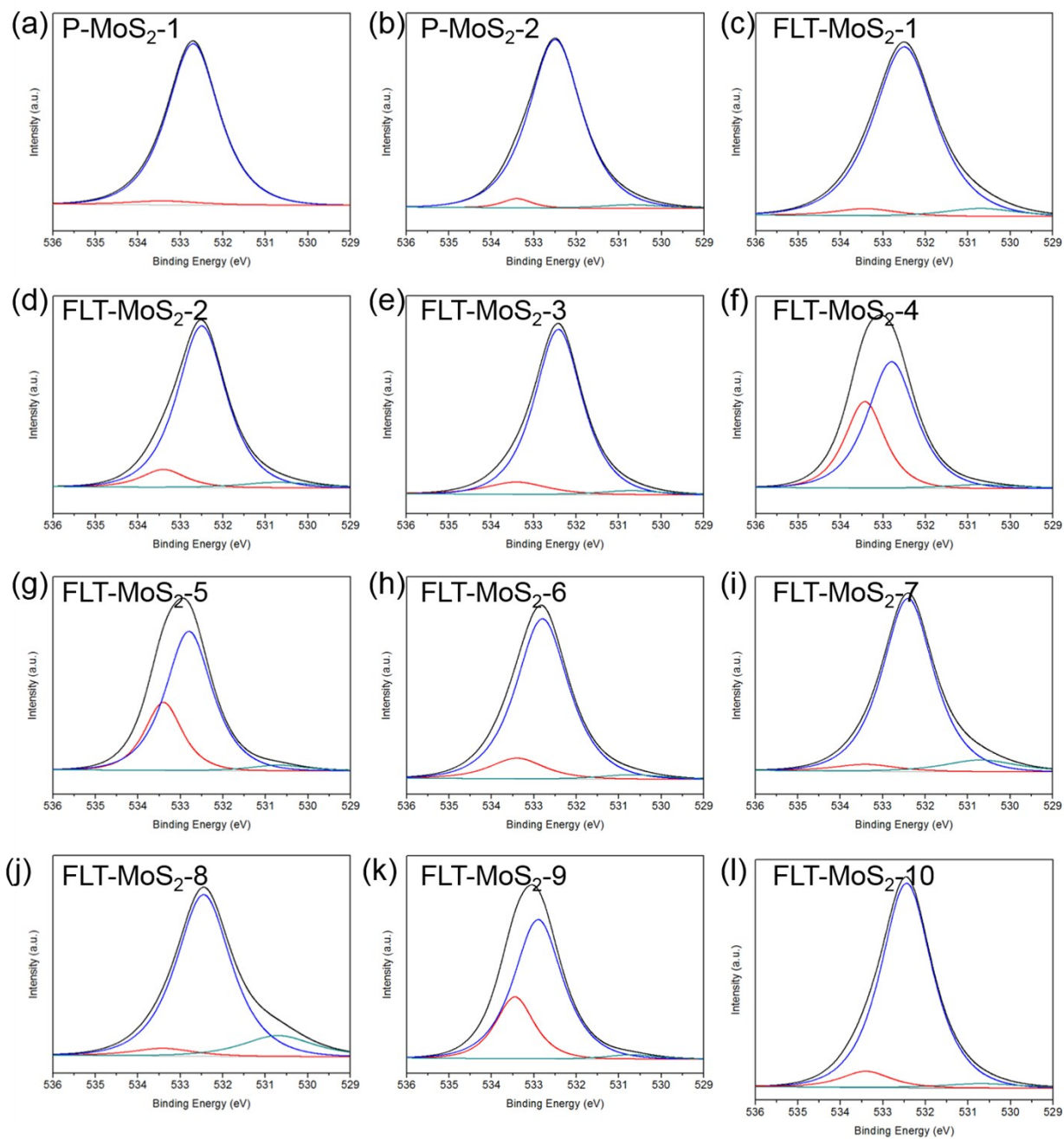


Fig. S11 More XPS O spectra of 2 P-MoS₂ and 10 FLT-MoS₂ samples. The red, blue, and cyan lines refer to O₂/MoS₂ Si-O, and O-Mo peaks, respectively.

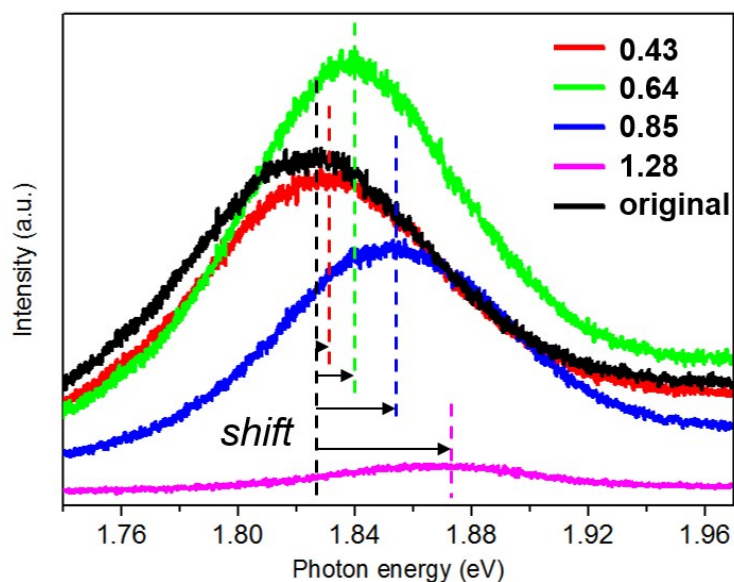


Fig. S12 PL spectra of FLT-MoS₂ under the variation of laser fluence (data for Figure 4f). Black line is the curve of P-MoS₂ (non-treated, pulse energy=0), and color lines are the curves of FLT-MoS₂ (the number is laser fluence, J/cm²). Scan velocity was 500 $\mu\text{m/s}$ and pulse delay was 0 ps.

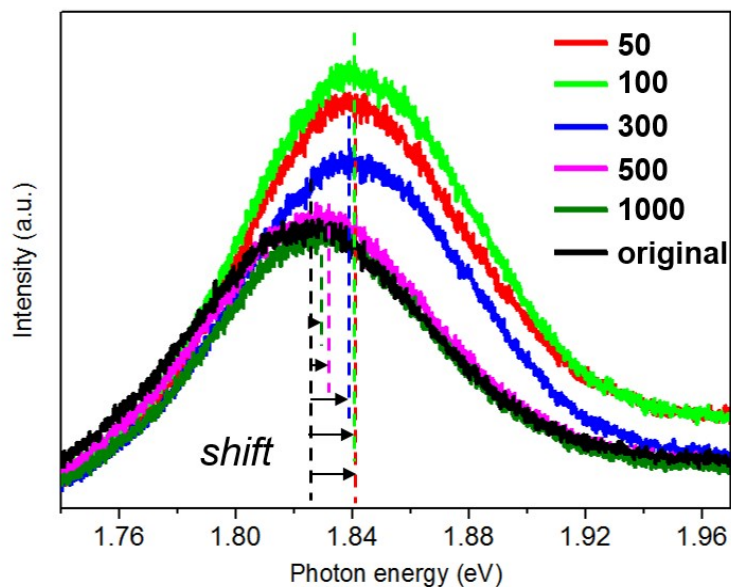


Fig. S13 PL spectra of FLT-MoS₂ under the variation of laser pulse scan velocity (data for Figure 4g). Black line is the curve of P-MoS₂, and color lines are the curves of FLT-MoS₂ (the number is pulse scan velocity, $\mu\text{m/s}$). Laser fluence was 0.43 J/cm² and pulse delay was 0 ps.

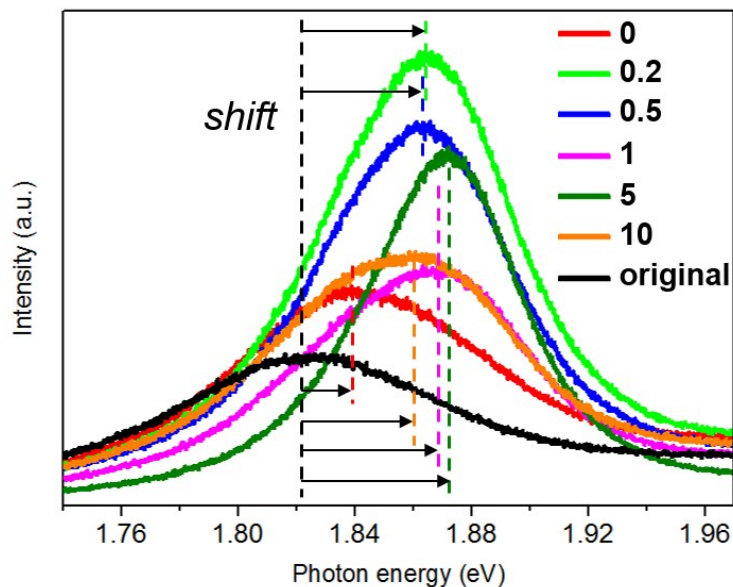


Fig. S14 PL spectra of FLT-MoS₂ under the variation of laser pulse delay (data for Figure 4h). Black line is the curve of P-MoS₂, and color lines are the curves of FLT-MoS₂ (the number is pulse delay, ps). Laser fluence was 0.43 J/cm² and scan velocity was 300 μm/s.

Explanation for the more obvious modification effect of TSFLT-MoS₂ than that of CFLT-MoS₂. This might be attributed to two detailed aspects. 1) Under the excitation by first subpulse of TSFL, MoS₂ was ionized and free electrons were generated, and subsequently the excited electrons–holes would recombine; the residual ionized-electrons by first subpulse can enhance the photon absorption for the second subpulse of TSFL,¹ before the accomplishment of electron–hole recombination (picosecond timescale),² they were again excited by second subpulse, and recombination was interrupted; hence under the excitation by TSFL, MoS₂ was ionized out more free electrons when comparing with the excitation by CFL. 2) Optical bandgap of P-MoS₂ was ~1.9 eV, hence MoS₂ was excited and damaged by femtosecond laser (λ=800 nm, photon energy≈1.55 eV) through a TPA process; however, the ionization of more free electrons of MoS₂ can result in the breaking of more chemical bonds and generation of more preliminary atoms vacancy which can induce additional/middle electronic states in MoS₂ energy gap (bandgap became narrow, shown as Figure 3), hence can lead to possible single-photon absorption of MoS₂ for subsequent pulses, which had higher photon absorption efficiency and can make electron heating faster, future inducing more Mo–S bonds breaking. Hence the integral photon absorption efficiency of MoS₂ under the irradiation of TSFL was higher than that under the irradiation of CFL and more defect/active sites were induced by TSFL.

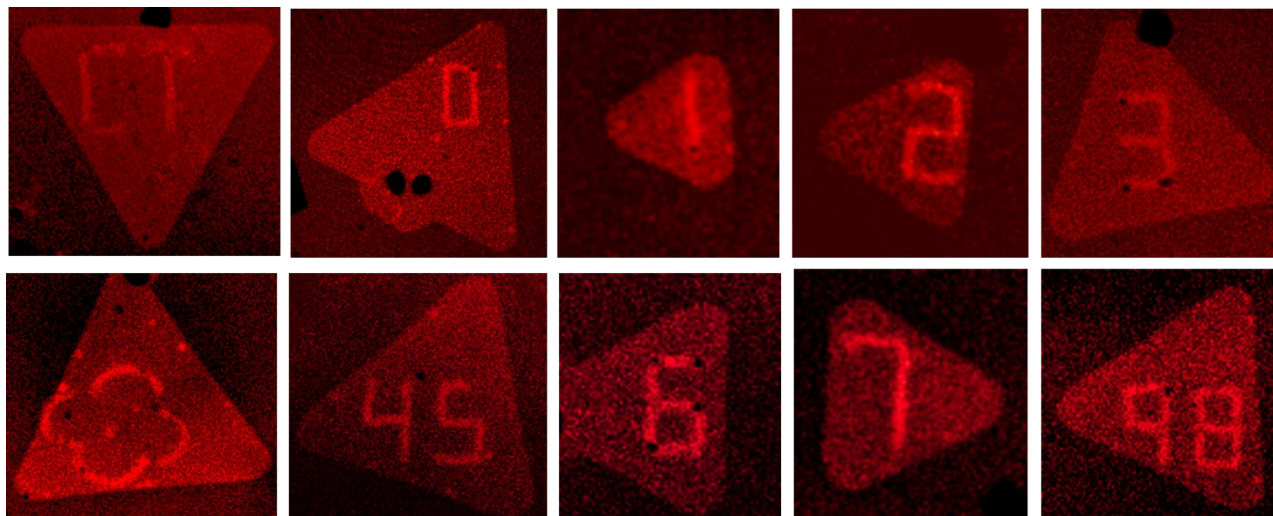


Fig. S15 More colorful PL micropatterns created on MoS₂ flakes. In a PL micropattern image, the surrounding black region is substrate, the triangular red region is the MoS₂ flake, and the bright red letters and symbols are the trace scanned by femtosecond laser direct writing.

Table S2 Raman frequencies (cm⁻¹) and assignments of the main bands of R6G.

Raman shift (cm ⁻¹)	Band assignment ³⁻⁷
613	C-C-C in-plane bending vibration
774	C-H out-plane bending vibration
1181	C-H and N-H bending vibrations
1310	C=C stretching vibration
1363	C-C stretching vibrations
1509	C-C stretching vibrations
1574	C=O stretching vibrations
1649	C-C stretching vibrations

References

1. M. Zhao, J. Hu, L. Jiang, K. Zhang, P. Liu and Y. Lu, *Sci. Rep.*, 2015, **5**.
2. H. Wang, C. Zhang and F. Rana, *Nano Lett*, 2015, **15**, 339-345.
3. Y. Q. Wang, S. Ma, Q. Q. Yang and X. J. Li, *Applied Surface Science*, 2012, **258**, 5881-5885.
4. C. D'Andrea, F. Neri, P. M. Ossi, N. Santo and S. Trusso, *Nanotechnology*, 2009, **20**, 245606.
5. L.-B. Luo, L.-M. Chen, M.-L. Zhang, Z.-B. He, W.-F. Zhang, G.-D. Yuan, W.-J. Zhang and S.-T. Lee, *J. Phys. Chem. C*, 2009, **113**, 9191-9196.
6. Z. Zenghui, X. Jian, H. Fei, L. Yang, C. Ya, S. Koji and M. Katsumi, *Japanese Journal of Applied Physics*, 2010, **49**, 022703.

7. P. Zuo, L. Jiang, X. Li, B. Li, Y. Xu, X. Shi, P. Ran, T. Ma, D. Li and L. Qu, *ACS Appl. Mater. Interfaces*, 2017, **9**, 7447-7455.